Published in Proc. Conf: *Noise in Complex Systems and Stochastic Dynamics,* eds. L. Schimansky Geier, D. Abbott, and C. Van den Broeck, SPIE vol. 5114, 2003, pp 372-382.

Solution of the boundary value problem for nonlinear flows and maps

Stefano Beri[a], Dmitri G. Luchinsky[a], Alexander Silchenko[a] and Peter V.E. McClintock[a]

[a] Department of Physics, Lancaster University, Lancaster LA1 4YB, UK

ABSTRACT

Fluctuational escape via an unstable limit cycle is investigated in stochastic flows and maps. A new topological method is suggested for analysis of the corresponding boundary value problems when the action functional has multiple local minima along the escape trajectories and the search for the global minimum is otherwise impossible. The method is applied to the analysis of the escape problem in the inverted Van der Pol oscillator and in the Henon map. An application of this technique to solution of the escape problem in chaotic maps with fractal boundaries, and in maps with chaotic saddles embedded within the basin of attraction, is discussed.

Keywords: Stochastic non linear dynamics, boundary value problem, heteroclinic trajectory, activation problem, topology of invariant manifold

1. INTRODUCTION

The motion of a dynamical system subject to noise typically consists of small fluctuation about an attractor of some kind. Their amplitude is typically of the order of $\sqrt{\epsilon}$, where ϵ is the intensity of the noise. On rare occasions, however, the system may make a fluctuation whose amplitude is much larger than $\sqrt{\epsilon}$. In this case the system is said to perform a *large fluctuation*.

Even though they are rare, large fluctuations are responsible for most of the important events that occur in stochastic nonlinear systems. In particular large deviations are involved in stochastic resonance,[4] directed diffusion in stochastic ratchets,[?,5,6] nucleation in electrochemical systems,[7] the dynamics of VCSELs[9,11,12] and gas lasers,[19,20] and the passage of currents of ions through open ionic channels[?] in biological membranes. For this reason, a deeper understanding of fluctuations and activation processes is much to be desired in relation both to continuous flows[1–3,8–10] and to maps.[13–20] Many promising steps towards a solution have been taken in the limit of zero noise intensity $\epsilon \to 0$. In this regime, the probability density for the system may be written in the asymptotic form[23]

$$\varrho(x,t) = z(x,t) \exp\left(-\frac{S(x,t)}{\epsilon}\right), \quad \epsilon \to 0. \tag{1}$$

In this limit, the escape probability is exponentially dominated by an "activation energy"* $S(x,t)$. The prefactor $z(x,t)$ contains next-to-the-leading order correction in the activation energy which take account of contributions due to a finite value of ϵ.

It follows from this asymptotic analysis[23,40] that the activation energy satisfies an Hamilton-Jacobi equation for a classical action.

$$\frac{\partial S}{\partial t} + H\left(\frac{\partial S}{\partial x}, x\right) = 0. \tag{2}$$

The action $S(x,t)$ can be computed explicitly along the trajectories by solution of the corresponding Hamilton's Equations. In a generic system, more than one trajectory of (2) terminates in the same final point (x,t). For this reason, the activation energy $S(x,t)$ is generally a multivalued function of position in the coordinate space.[2,6,21,25–35] The trajectory reaching the boundary that has the least possible energy is known as the *most*

*For a non equilibrium system, the potential S is not an energy; but, in what follows, the quotation marks will be omitted.

probable escape path (MPEP) and the corresponding value of the energy gives the activation potential. The MPEP is an heteroclinic trajectory emanating from the initial state at $t \to -\infty$ and reaching the final state at $t \to +\infty$. For non trivial system, solution of this boundary value problem is in practice very complicated. The difficulties increase with the dimension of the system and a successful application cannot be relied upon in any general case. This imposes strong limitations, for example, in applying the method to study of escape from a chaotic attractor in the problem of control of chaos.[38] A similar asymptotic analysis has been proposed[16–18,39] to investigate activation precesses in stochastic maps of the form

$$x_{n+1} = f(x_n) + \xi_n, \tag{3}$$

where x_n describes the state of the system, $f(x)$ is a nonlinear function and ξ_n is a set of white Gaussian variables satisfying $\langle \xi_n \xi_m \rangle = \epsilon \delta_{mn}$. The asymptotic $\epsilon \to 0$ solution of the escape problem requires minimisation of the activation energy

$$E = \frac{1}{2} \sum \xi_n^2 \tag{4}$$

and the calculation of a MPEP analogous to that for continuous systems. The minimisation is performed using the method of Lagrangian multipliers.[17,18] As a result (3) is transformed in an extended area-preserving map, and the activation energy can be calculated along the solutions. The structures of the invariant manifolds and of the energy surface are again very complex, and the calculation of the MPEP for a generic non linear map is very difficult even for low dimension maps. In particular the determination of the MPEP becomes extremely hard in the case of chaotic saddles embedded in the basin of attraction[24]

In this paper we address the problem of activated processes in the limit $\epsilon \to 0$ for both nonlinear flows and maps. In particular we consider noise induced escape for continuous systems exhibiting a saddle cycle, and of noise induced escape from a smooth boundary of a domain of attraction in nonlinear maps. We perform a topological investigation of the invariant manifold and we show how such an analysis substantially simplifies the solution of the boundary value problem. We introduce a way of parameterising the escape trajectories on the unstable manifold, and we consider the action (or the activation energy) at the escape instant as a function of these parameters. The global minimisation of the action in relation to these parameters gives us the lowest energy solution of the boundary value problem. The multiplicity of solutions of the boundary value problem is also addressed. In particular we show how, in principle, all possible solutions of the boundary value problem (i.e. including unphysical ones) can be obtained. To show explicitly how the method works, we choose two different systems: the inverted Van der Pol oscillator and the Henon map. The results for the activation energy and for the escape trajectories are shown to agree with the experimental values obtained with numerical simulations.

The paper is structured as follow: in Sec. 2 we present the problem of escape for a continuous system. The asymptotic analysis of the Fokker-Planck equation is performed, and the auxiliary Hamiltonian system is introduced for the calculation of the activation energy. The structure of the invariant manifolds in the extended phase space is discussed, including their singularities and the kind of trajectories generating them. In Sec. 2.2 we introduce the action plot as a tool to investigate activation problems from the topological viewpoint. In Sec. 3 we apply the method to solve the particular problem of escape in the inverted Van der Pol oscillator. Finally in Sec. 4 we study the Henon map as an example of the application of the method to a non linear map. In both Sec. 3 and 4, theoretical results obtained using the action plot are shown to be in agreement with experimental results from numerical simulations.

2. NOISE-INDUCED ESCAPE

Consider a dissipative dynamical system under the influence of noise, described by a Langevin equation of form

$$\dot{x}_i = K_i(\vec{x}) + \sqrt{\epsilon}\sigma_{ij}\xi_j(t). \tag{5}$$

Here $\xi_j(t)$ are Gaussian, zero-mean, uncorrelated sources of noise. They are linearly mixed by the noise matrix σ_{ij}. The parameter ϵ is again the intensity of the noise, and it is the small parameter in the theory. We consider noise-induced escape from a planar domain Ω with an attracting fixed point S and a smooth boundary $\partial\Omega$. One

example of such a system is provided by the inverted Van der Pol oscillator (IVDP) in the presence of noise, for which

$$\begin{cases} \dot{x}_1 = x_2 \\ \dot{x}_2 = -2\eta(1-x_1^2)x_2 - x_1 + \sqrt{4\eta\epsilon}\xi_2(t) \end{cases} \tag{6}$$

The noise matrix for this system is $\sigma_{ij} = \sqrt{4\eta}\delta_{i2}\delta_{j2}$. The fixed point has coordinates $(0,0)$ and the smooth boundary is formed by an unstable cycle. The Fokker-Planck equation corresponding to Eq.(5) is

$$\frac{\partial \varrho}{\partial t} = \frac{\partial}{\partial x_i}\left(-\varrho K_i + \frac{\epsilon}{2}\frac{\partial}{\partial x_j}Q_{ij}\varrho\right), \tag{7}$$

where Q_{ij} is a diffusion matrix defined as

$$Q_{ij} = \sigma_{ik}\sigma_{jk}.$$

In the limit of $\epsilon \to 0$, (7) is solved via WKB expansion. Substitution of the approximation (1) into (7), and expansion in powers of ϵ, shows that to order $\frac{1}{\epsilon}$ (which is leading when $\epsilon \to 0$) the function $S(x,t)$ satisfies the following partial differential equation[23,40]

$$\frac{\partial S}{\partial t} + K_i\frac{\partial S}{\partial x_i} + \frac{1}{2}Q_{ij}\frac{\partial S}{\partial x_i}\frac{\partial S}{\partial x_j} = 0. \tag{8}$$

Eq.(8) may be expressed as an Hamilton-Jacobi (2) for an auxiliary Hamiltonian dynamical system with the Hamiltonian

$$H(x,p) = K_i p_i + \frac{1}{2}Q_{ij}p_i p_j, \quad p_i \equiv \frac{\partial S}{\partial x_i}. \tag{9}$$

The system of Hamiltons equations corresponding to (9) is

$$\begin{cases} \dot{x}_i = K_i + Q_{ij}p_j, \\ \dot{p}_i = -\frac{\partial K_j}{\partial x_i}p_j \\ \dot{S} = \frac{1}{2}Q_{ij}p_i p_j, \end{cases} \tag{10}$$

where $S(\vec{x},t)$ can be interpreted as an action in the context of classical mechanics.[41,42] The matrix Q_{ij} is positively defined, so that S is nondecreasing along solutions of (10) emanating from the initial stationary state. Moreover, $S(x,t)$ is differentiable almost everywhere in the coordinate space. For these reasons S is a Lyapunov function and can be used as nonequilibrium thermodynamic potential to describe the fluctuating system.[25,27,28] The trajectory emanating from the initial steady point that reaches a final point with the least action is called *optimal*. Trajectories differing from optimal can reach the same final point with higher action. They correspond to other local extrema of the action functional. Their contribution to the probability density $\varrho(x,t)$ is exponentially small for $\epsilon \to 0$ and the probability distribution is dominated by the global minimum. The concept of optimal trajectories is not just a mathematical abstraction: the prehistory of a large fluctuation is sharply peaked about the optimal path solution of (10). Optimal paths have been observed in both numerical simulations and analogue experiments[33,43,44] and in the dynamics of activated escape in a semiconductor laser.[45]

In the case of a noisy map of the form (3), an extended map is obtained in a similar way. Minimising the activation energy (4) with respect to the set $\{\xi_n\}$ with the condition (3) is equivalent to minimising the auxiliary function[17,18]

$$F(x_n,\xi_n,\lambda_n) = \sum\left(\frac{1}{2}\xi_n^2 + \lambda_n\Big(x_{n+1} - f(x_n) - \xi_n\Big)\right) \tag{11}$$

with respect to $\{x_n\}$, $\{\xi_n\}$ and $\{\lambda_n\}$. The auxiliary variable λ_n is known as a Lagrange multiplier. The minimisation leads to an area preserving map for the variables $\{x_n\}$ and $\{\lambda_n\}$ and to the equation for the evolution of the activation energy.

$$\begin{cases} x_{n+1} = f(x_n) + \lambda_n \\ \lambda_{n+1} = \left(\frac{\partial f}{\partial x}\big|_{x_{n+1}}\right)^{-1}\lambda_n \\ E_{n+1} = E_n + \frac{1}{2}\lambda_n^2. \end{cases} \tag{12}$$

The two systems (10) and (12) are completely analogous. As in the case of continuous systems, the stable and unstable orbits for system (3) become saddle orbits in the extended system (12). In what follows, we will consider the particular case of a map presenting a stable period-one orbit x_s and smooth (non-fractal) basin boundaries, and we address the problem of noise activated escape from the basin of attraction.

2.1 Heteroclinic trajectories

In the extended phase space $x - p$, the extreme paths emanating from a fixed point (at $t \to -\infty$) of the deterministic flow defined by the Hamiltonian equations (9) span the unstable Lagrangian manifold (LM) of this point.[36,40,42,46] In a generic n-dimensional system, the phase state is $2n$-dimensional and the manifold is n-dimensional. The trajectories solution of (10) form an $(n-1)$-parameter family on the unstable manifold, and every point on the LM is completely determined, giving the initial conditions at a given initial time t_0 for the trajectory reaching that point at time t. In a small neighbourhood of the fixed point, the action may be written in the form

$$S(x,t) = \frac{1}{2} W_{ij} \delta x_i \delta x_j \tag{13}$$

where δx_i is the deviation from the stable point in the x_i direction and W_{ij} is the $(n \times n)$Hessian matrix of the action calculated for the stable point. The LM in a small neighbourhood of the fixed point is an n-dimensional linear subspace completely defined by the equation

$$p_i = W_{ij} \delta x_j. \tag{14}$$

In a planar system, the 2-dimensional LM can be parameterised using the following procedure: the initial conditions in the coordinate space are taken on a small circle of radius r_0. Then using Eq. 13 and 14 the corresponding momenta and action are found. In higher dimensional systems, more parameters are required to parameterise the manifold, but the same general procedure still applies: parameterising the coordinate space in a small neighbourhood of the fixed point, and using 13 and 14 to obtain the momenta and the action. Similar parameterisations are possible when the steady state is limit cycle and not a stable point. Differentiating Eq. 2 twice the following Riccati equation for the coefficients W_{ij} is obtained[31]

$$\frac{d}{dt} W_{ij} = -\frac{\partial^2 H}{\partial x^i \partial x^j} - W_{ik} \frac{\partial^2 H}{\partial p^k \partial x^j} - W_{jl} \frac{\partial^2 H}{\partial x^i \partial p^l} - W_{jl} W_{ik} \frac{\partial^2 H}{\partial p^k \partial p^l}. \tag{15}$$

In the case of a fixed point this equation reduces to an algebraic equation. In the case of a limit cycle, (15) has to be solved along the limit cycle with the additional "periodicity" constraint $W_{ij}(l) = W_{ij}(l + L)$ where l is a coordinate along the cycle and L is the total length of the cycle.

Another invariant manifold is the stable manifold spanned by the trajectories converging to the final steady state for $t \to +\infty$.

The same picture applies to the case of stochastic maps. This is particularly clear in the case of maps obtained as Poincaré sections from continuous flows. Due to the discreetness of time, trajectories emanating at $t \to \infty$ for a n-dimensional map are an n parameter family on the unstable manifold. In a small neighbourhood of the steady state, a linear relationship among the coordinates and "momenta" λ analogous to (14) can be written

$$\lambda_i = A_{ij} \delta x_j. \tag{16}$$

Since no Hamilton-Jacobi equation can be written in the case of maps, the coefficients A_{ij} have to be computed directly by a linearisation of 12. Consider the case of an n-dimensional map and a base $\vec{v}_1 \dots \vec{v}_n$ for its unstable manifold. A generic vector on the unstable manifold is then written as a linear combination of the base vectors

$$\begin{pmatrix} x_1 \\ \vdots \\ x_n \\ \lambda_{x_1} \\ \vdots \\ \lambda_{x_n} \end{pmatrix} = \sum_i \alpha_i \begin{pmatrix} v_{ix_1} \\ \vdots \\ y_{ix_n} \\ v_{i\lambda_{x_1}} \\ \vdots \\ v_{i\lambda_{x_n}} \end{pmatrix} \tag{17}$$

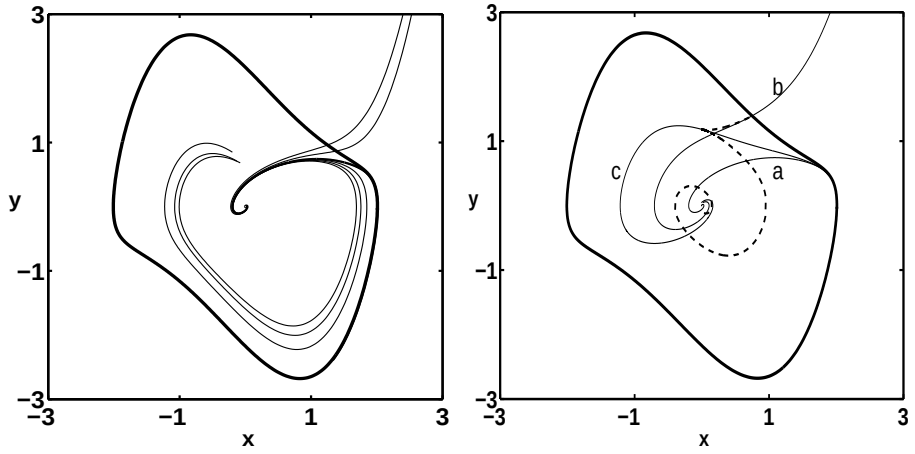

Figure 1. Left: A heteroclinic trajectory (bold curve) for the inverted van der Pol system and the trajectories (thinner curves) resulting from small perturbations about it. Non-heteroclinic trajectories may cross the cycle and go far away, or they may be reflected back toward the internal regions of the limit cycle and, after that, fluctuate again. The η parameter is 0.5. Right: Significant trajectories in the pattern: a the MPEP; b the trajectory corresponding to the top of the first hill in the action plot, which touches the cycle and the caustic at the same moment; c another (non-optimal)heteroclinic path. Trajectory c passes exactly through the cusp.

where $\alpha_1 \ldots \alpha_n$ are n real parameters. The values of the parameters $\alpha_1 \ldots \alpha_n$ can be obtained from the first n equations in (17). Substituting the values of the parameters in the other n equations in (17), the desired linear relation (16) among the coordinates and momenta is obtained. In a 2-dimensional map, the manifold is parameterised in a similar way to that used in continuous systems: the initial conditions are chosen between two circles whose radii are chosen so as to include all possible trajectories in the pattern.

It is clear that a trajectory emanating from the first steady state and converging to the second one lies on the intersection of these two manifolds; it is a *heteroclinic trajectory* (HT)[47] of (9). Since both the initial and final state are invariant sets of the original noise-free system (5), the heteroclinic trajectory has zero momentum at $t \to \pm\infty$. In Fig. 1 the heteroclinic trajectory in the inverted van der Pol system, and small perturbations about it, are shown by the thick and thin full lines respectively. The HT converges to the limit cycle, whereas trajectories that are small perturbations of the HT show either of two possible types of behaviour: they may cross the cycle and escape to infinity; or they may be reflected back into the internal region. The HT separates these two classes of trajectories (cf. the discussion in[32]).

Outside the linear regime, the structure of the Lagrangian manifolds becomes more complicated.[28,36,46] In particular, the pattern of escape trajectories in the coordinate space shows multiple intersections. In a continuous planar system with a saddle cycle, the MPEP and its small perturbations move close to the cycle, and necessarily intersect the trajectories that are going to infinity (See Fig. 1). The projection of the LM onto the coordinate space contains singularities away from the initial state.[25,28,29,36,46] For a two dimensional Lagrangian manifold (such as in the Van der Pol system) the only structurally stable types of singularity are the *fold* and the *cusp*.[42] In projection, folds lead to caustics and cusps lead to cusp points.[25,28,29]

A cusp point separates a caustic into two different branches that emanate from it: an external one (that crosses the cycle) and an internal one. The external branch is generated by trajectories moving toward the cycle (having essentially non-zero momentum p), whereas the internal one is generated by trajectories that have been reflected from the cycle and are moving back toward the origin.

It is a general result that, in a system with saddle cycles, the internal branch of the caustic converges to the steady state. Indeed, the internal branch is generated by trajectories moving back to the internal region of the cycle after being reflected by the saddle cycle. The momentum on the HT trajectory is asymptotically zero (for $t \to \infty$) and the closer the trajectory approaches to the HT the smaller is its momentum. Consequently trajectories that are very weak perturbations of the HT have very small momenta p.[31] The smaller the momentum

of the trajectory, the closer it is to the purely relaxational trajectory (i.e. a trajectory that has $p = 0$ by definition) on its way back to the interior of the limit cycle, and the closer this trajectory approaches the steady state before touching the caustic. Thus, the caustic converges to the stationary state. However, trajectories with non-zero momentum belong to the unstable Lagrangian manifold of the steady state. Therefore these trajectories cannot touch the steady state. Instead, they will be reflected by the internal branch of the caustic and then move back to the saddle cycle. On the other hand, topological analysis shows[31,43,46] that, in regions of folding, the Lagrangian manifold has three different sheets: two external sheets and one internal. A trajectory emanating from the steady state stays on one of the external sheets. After being reflected by the caustic it moves to the internal sheet of the LM. Once a trajectory is on the internal sheet of the LM, it stays there forever[36] because of the Cauchy's Theorem. Thus trajectories reflected by the internal branch of the caustic, moving back to the saddle cycle, must stay on the internal sheet of the LM. Close to the saddle cycle these trajectories will repeat the same pattern of behaviour as was described above. Some of them will cross the cycle, while the others will be reflected from the cycle, and these two types of behaviour will be separated by a new heteroclinic trajectory that approaches the saddle cycle at $t \to \infty$. Consequently, they will repeat the pattern of intersections related to another folding of the LM. In conclusion, the central sheet of the LM will experience multiple stretchings and foldings (cf.[31,48]). An infinite number of heteroclinic trajectories is produced in this way. Corresponding to folding in the LM, in the action surface swallow tail singularities appear.[36] The middle sheet of the LM corresponds in this case to the top sheet of the action surface. Subsequent multiple folding of the middle sheet of the LM induces a complex structure of swallow tail singularities in the action surface.

2.2 The action plot and its structure

In this section we introduce the new technique for solution of the boundary value problem. As discussed above, the optimal trajectories on the LM are an $(n-1)$-parameter family (for a continuous flow, or n-parameters for a map), where n is the dimensionality of the system. The space of parameters is diffeomorph to a torus $S^1 \times \ldots \times S^1$. For example, in the IVDP system, the space of parameters is a simple S^1, as it appears explicitly from the choice of parameterisation discussed in Sec.2; for a 2-dimensional system the space of parameters is a torus $S^1 \times S^1$. The evolution of the trajectories corresponding to any point in the parameter space is followed until the escape is realised. The value of the activation energy (action) at the escape is recorded. In this way we build a function

$$S: \; S^1 \times \ldots \times S^1 \longrightarrow \mathbb{R}.$$

We will refer to this result as the *action plot*. In order to show how the action plot can help to solve the boundary value problem for activated processes, we consider the simple case of the IVDP system. The action plot is shown in Fig. 2. It is immediately evident that the value of the action at the limit cycle is a complex discontinuous function of the parameter. The plot consists of a set of "hills" of different height separated by discontinuities in the action. The two large hills of lowest action are identical on account of the symmetry of the Van der Pol equations. The discontinuities in action at the edges of the hills correspond to heteroclinic paths, which can be appreciated as follows. As we have discussed above, weak perturbations of the HT are separated into two sets of trajectories: those that cross the cycle and those that are reflected back. The change from one type of behaviour to the other occurs abruptly with continuous change of the parameter. On the other hand, it can be seen from Eq. (10) that the action is a non-decreasing function along the path and its evolution is determined by the behaviour of p^2. Consequently, in the vicinity of the limit cycle (where p tends to zero), small perturbations of the HT have actions very close to that of the HT itself. Thus the action varies smoothly with the parameter for the first set of trajectories that cross the limit cycle as soon as they deviate from the HT. Trajectories that are reflected by the limit cycle, on the other hand, acquire a finite additional value of action before they return to the vicinity of the limit cycle. Consequently, the action plot exhibits a discontinuity every time the parameter passes through the critical value corresponding to the HT: we infer there must be infinitely many discontinuity points in the action plot for a system with a limit cycle. This "hill-peak" structure does not depend on the explicit choice of parameterisation: it is a property that depends on the topology of the pattern of optimal trajectories. Study of the action plot allows us to determine the initial condition corresponding to heteroclinic trajectories. Moreover, choosing initial conditions corresponding to peaks, it is possible to investigate the trajectories in the central sheet of the fold. The value for the activation energy is obtained as the minimum of the action plot. The multiple, mutually enclosing, folds of the LM result in an infinite number of heteroclinic trajectories. This structure can

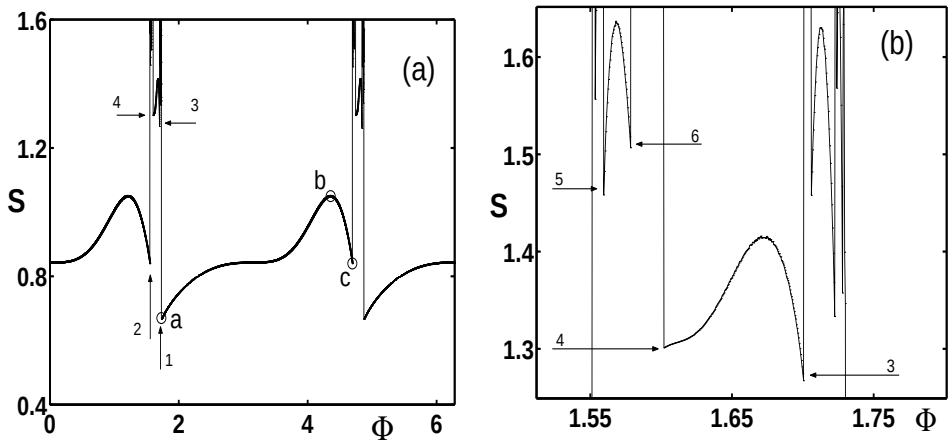

Figure 2. (a) The action plot for escape in the IVDP system ($\eta = 0.5$). The plot shows a very complex structure made up of rounded "hills" and sharp "peaks". Some of the discontinuity points are numbered (see text). The first peak is bounded at $\Phi_1 = 1.73$ and $\Phi_2 = 1.55$; inside the peak a second hill is visible with edges at $\Phi_3 \sim 1.70$ and $\Phi_4 = 1.60$. (b) A zoom of the plot around this second hill shows how this structure repeats itself inside the hills: on the sides of the second hill other hills are visible. Considering for example the left-hand hill, we can observe a third hill with edges at $\Phi_5 \sim 1.56$ and $\Phi_6 \sim 1.59$. The same structure also exists in the right-hand peak.

clearly be seen in the action plot. Thus the hill of low action is surrounded by regions of discontinuity (see Fig. 2(a)) in the action function. They correspond to the set of trajectories reflected from the limit cycle by the HT with the initial condition ϕ_1 (and $\phi_1 + \pi$). This set is bounded by a second HT with initial condition ϕ_2 (and $\phi_2 + \pi$). The same structure repeats itself for the set of initial conditions between ϕ_2 and ϕ_1: a hill bounded by heteroclinic trajectories with initial conditions ϕ_3 and ϕ_4 can be seen in Fig.2(b). Significant trajectories in the first hill are shown in Fig.1 on the right: the two heteroclinic paths a and c correspond to the edges of the first hill. Trajectory a provides the global minimum of the action. Trajectory b touches simultaneously the caustic and the cycle; it corresponds to the maximum of the first hill. The same structure repeats itself in each of the upper hills. We conclude that the action plot reveals a self-similar structure of mutually enclosed multiple folds of the LM, and it allows us to identify initial conditions corresponding to significant points of the structure, including those corresponding to the initial conditions of the heteroclinic trajectories. This enables us, at least in principle, to find all the HTs in the system.

In higher dimensional parameter spaces, the the picture is more complex. Nevertheless, the following general results hold. Regions of significantly different action (peaks in the 1D case) are well separated from one and other by discontinuity surfaces which are connected in the parameter torus. The trajectory corresponding to the minimum action is the heteroclinic trajectory which realises the escape.

3. NOISE-INDUCED ESCAPE IN THE INVERTED VAN DER POL OSCILLATOR

As our first application, we study the activation energy for noise-induced escape in the inverted Van der Pol oscillator (6). The parameter η in (6) regulates both friction (which is related to the noise intensity via the fluctuation-dissipation theorem[49]) and the pumping of energy into the system. As a result, this systems displays a nontrivial dependence of activation energy on the value of η. As mentioned above in the introduction, noise-induced escape from the basin of attraction of the fixed point is governed by the properties of the most probable escape path, which is the heteroclinic trajectory of lowest action. Accordingly, the action plot can be used to find the activation energy of systems with limit cycles. The most probable escape path is simply the path corresponding to the discontinuity point of lowest action in the action plot. The value of action at this point gives the activation energy. Other heteroclinic paths can also be found easily from the action plot. In Fig. 4 the theoretical dependence of S on η (full curve) is compared with Monte Carlo simulations (crosses) in the limit of small noise intensity. The theoretical predictions and results of the simulations agree well over a wide

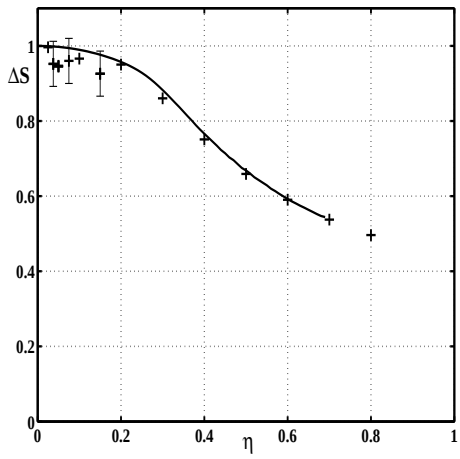

Figure 3. The activation energy for escape in the inverted van der Pol oscillator as a function of η. The results of Monte Carlo simulations (crosses) are compared with the theory (full curve).

range of parameter values. The small-η-asymptotic behaviour of the activation energy corresponds to theoretical predictions based on adiabatic elimination of the fast variables. The value $\eta = 0$, corresponding to deterministic motion of the system, may be approached only as a limit.

4. NOISE-INDUCED ESCAPE IN THE HENON MAP

Consider, as our second specific example, the noise-driven Henon map

$$\begin{cases} x_{n+1} = a - x_n^2 + by_n + \xi_n \\ y_{n+1} = x_n. \end{cases} \tag{18}$$

Here x_n and y_n are the dynamical variables; a and b are parameters of the system and $\{\xi_n\}$ is a set of uncorrelated white Gaussian noises of intensity ϵ. The parameters are tuned for the system to exhibit a stable period-1 orbit and an attractor at infinity. The boundary of the basins of attraction is smooth, with a period-1 saddle orbit. For this particular map the extended system (12) is

$$\begin{cases} x_{n+1} = a - x_n^2 + by_n + \lambda_{xn} \\ y_{n+1} = x_n \\ \lambda_{xn+1} = \lambda_{yn} \\ \lambda_{yn+1} = \frac{\lambda_{xn} + 2x_{n+1}\lambda_{xn}}{b} \end{cases} . \tag{19}$$

The activation process takes place in two parts: noise driven motion from the period-1 cycle to the boundary; and noise free motion along the boundary.

5. CONCLUSIONS

Our analysis shows how it is possible to use the action plot to simplify the solution of the boundary value problems arising in the framework of non-equilibrium activated processes. In particular, our analysis proved to be a convenient framework within which to study noise induced escape via an unstable limit cycle in planar systems, and through the boundary of the basin of attraction for nonlinear maps. Besides the van der Pol and Henon systems described in this paper, we have successfully applied this technique to find the frequency and amplitude dependence of the activation energy for a periodically driven overdamped Duffing oscillator, and to solve the boundary value problem for the Holmes map in the case of smooth and fractal boundaries. We have demonstrated that both the topological analysis of the global behaviour of the unstable LM of the fixed point, and the solution of the boundary value problem, can be substantially simplified by use of this representation. We applied the technique to find the heteroclinic trajectories of lowest action in the inverted Van der Pol oscillator as

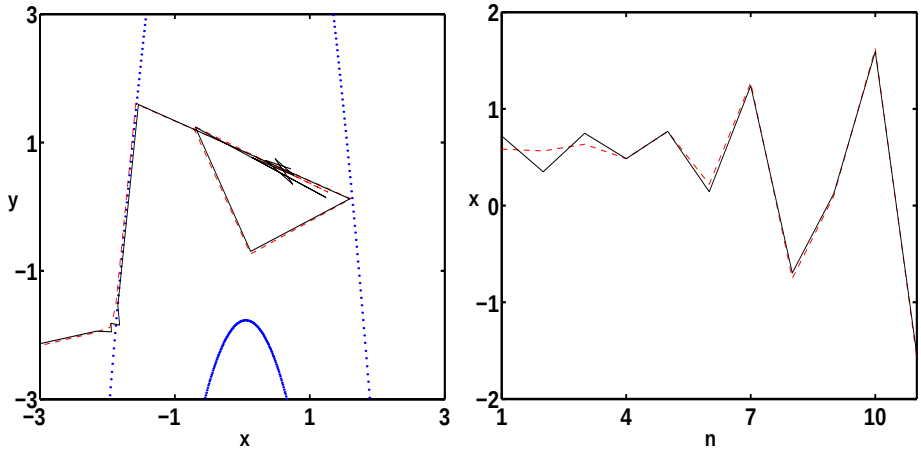

Figure 4. Comparison of theory and experiments for the escape problem in the Henon map (parameters are $a = 1.1$ and $b = -0.3$). Theoretical MPEP (dashed) and numerical escape path (full line) are plotted in coordinate domain (left) and iterations-coordinates domain (right). Theory and simulations perfectly agree. The escape takes place through the saddle point in $(-1.88; -1.88)$

a function of the damping parameter η. The activation energy found in this way is in a good agreement with the results of Monte Carlo simulations over a wide range of values of the parameter η. The method can in principle be applied to locate all possible heteroclinic trajectories (i.e. including non-optimal ones). A slightly modified version of the technique has been applied to successfully solve the boundary problem for the Henon map.

The path that minimises the action is in near perfect agreement with the results of the simulations. The same technique has been applied for a range of maps, including the case of a period 4 initial orbit with fractal boundaries, the escape from the basin of attraction of a chaotic attractor[50] or escape for the case of a chaotic saddle embedded in the basin of attraction.[24]

REFERENCES

1. R. S. Maier and D. L. Stein, Phys. Rev. Lett. **77**, 4860 (1996).
2. V. N. Smelyanskiy, M. I. Dykman, and B. Golding, Phys. Rev. Lett. **82**, 3193 (1999).
3. J. Lehmann, P. Reimann, and P. Hänggi, Phys. Rev. Lett. **84**, 1639 (2000).
4. M. I. Dykman, D. G. Luchinsky, R. Mannella and P.V.E. McClintock, Nuovo Cimento D **17**, 661 (1995).
5. M. O. Magnasco, Phys. Rev. Lett. **71**, 1477 (1993).
6. M. I. Dykman, H. Rabitz, V. N. Smelyanskiy and B. E. Vugmeister, Phys. Rev. Lett. **79**, 1178 (1997).
7. V. N. Smelyanskiy, M. I. Dykman, H. Rabitz, B. E. Vugmeister, S. L. Bernasek and A. B. Bocarsly, J. Chem. Phys. **110**, 11488 (1999).
8. R. S. Maier and D. L. Stein, Phys. Rev. Lett. **86**, 3942 (2001).
9. M. B. Willemsen, M. P. van Exter and J. P. Woerdman, Phys.Rev.Lett **84** 4337 (2000).
10. M. B. Willemsen, M. P. van Exter and J. P. Woerdman, Phys.Rev.A **60** 4105 (1999).
11. M. P. van Exter, R. F. M. Hendriks and J. P. Woerdman, Phys. Rev. A. **57**, 2028 (1998).
12. M. P. van Exter, M. B. Willemsen and J. P. Woerdman, Phys. Rev. A. **58**, 4191 (1998).
13. H. P. Herzel and B. Pompe, Phys. Lett. A **122**, 121 ((1987).
14. H. Herzel, W. Ebeling and T. Schulmeister, Z. Naturforsch. **42a**, 136 (1987).
15. G. Meyer-Kress and H. Haken, J.Stat. Phys. **26**, 149 (1981).
16. P. Beale, Phys. Rev. A **40** 3998 (1989).
17. R. Graham, A. Hamm, T. Tél, Phys. Rev. Lett. **66** 3089 (1991).
18. P. Grassberger, J.Phys. A **22** 3283 (1989).
19. V. A. Gaisyonok, E. V. Grigorieva and S. A. Kashchenko, Opt.Commun. **124** 408 (1996).
20. V. N. Chizhevsky, E. V. Grigorieva and S. A. Kashchenko, Opt.Commun. **133** 189 (1997).

21. V. N. Smelyanskiy *et al.*, J. Chem. Phys. **110**, 11488 (1999).
22. J. Lehmann, P. Reimann, and P. Hänggi, Phys. Rev. E **62**, 6282 (2000).
23. M. Freidlin and A. D. Wentzel, *Random Perturbations in Dynamical Systems* (Springer, New-York, 1984).
24. S. Kraut and U. Feudel, Phys. Rev. E **67**, 015204 (2003).
25. R. Graham and T. Tel, Phys. Rev. Lett. **52**, 9 (1984).
26. R. Graham and T. Tel, Phys. Rev. A **31**, 1109 (1985).
27. R. Graham, in *Noise in Nonlinear Dynamical Systems*, edited by F. Moss and P. V. E. McClintock (Cambridge University Press, Cambridge, 1989), vol. 1, pp. 225–278.
28. H. R. Jauslin, Physica A **144**, 179 (1987).
29. M. V. Day, Stochastics **20**, 121 (1987).
30. P. Talkner, Z. Phys. B **68**, 201 (1987).
31. R. S. Maier and D. L. Stein, J. Stat. Phys. **83**, 291 (1996).
32. R. S. Maier and D. L. Stein, SIAM J. Appl. Math. **57**, 752 (1997).
33. M. I. Dykman, D. G. Luchinsky, P. V. E. McClintock, and V. N. Smelyanskiy, Phys. Rev. Lett. **77**, 5229 (1996).
34. V. N. Smelyanskiy, M. I. Dykman, H. Rabitz, and B. E. Vugmeister, Phys. Rev. Lett. **79**, 3113 (1997).
35. T. Naeh, B. Kłosek, M. M. Matkovsky, and Z. Schuss, SIAM J. Appl. Math. **50**, 595 (1990).
36. M. I. Dykman, M. M. Millonas, and V. N. Smelyanskiy, Phys. Lett. A **195**, 53 (1994).
37. M. I. Dykman *et al.*, Int. J. of Bifurcation and Chaos **8**, 747 (1998).
38. D. G. Luchinsky *et al.*, Int. J. Bifurcation and Chaos **12**, 583 (2002).
39. P. Grassberger, Phys. Rev. A **38**, 2066 (1988).
40. D. Ludwig, SIAM Rev. **17**, 605 (1975).
41. L. D. Landau and E. Lifshits, *Course of Theoretical Physiscs* (Pergamon, Oxford, 1976), Vol. 1.
42. V. Arnold, *Mathematical Methods of Classical Mechanics* (Springer-Verlag, Berlin, 1978).
43. M. I. Dykman *et al.*, Phys. Rev. Let. **68**, 2718 (1992).
44. D. G. Luchinsky, P. V. E. McClintock, and M. I. Dykman, Reports on Progress in Physics **61**, 889 (1998).
45. J. Hales, A. Zhukov, R. Roy, and M. I. Dykman, Phys. Rev. Lett. **85**, 78 (2000).
46. V. N. Smelyanskiy and M. I. Dykman, Phys. Rev. E **55**, 2516 (1997).
47. M. A. Lieberman and A. J. Lichtenberg, *Regular and Chaotic Dynamics* (Springer, New York, 1992).
48. M. V. Berry, in *Wave Propagation and Scattering*, edited by B. J. Uscinski (Clarendon, Oxford, 1986), pp. 11–35.
49. L. D. Landau and E. M. Lifshits, *Theoretical Physics: Statistical Physics* (Nauka, Moscow, 1972).
50. A. Silchenko, S. Beri, D. G. Luchinsky and P. V. E. McClintock, submitted to Phys. Rev. Lett.